Journal of Catalysis **185,** 170–181 (1999)
Article ID jcat.1999.2489, available online at http://www.idealibrary.com on IDEAL®

Temperature-Programmed Desorption of Hydrogen from Platinum Particles on γ-Al_2O_3: Evidence of Platinum-Catalyzed Dehydroxylation of γ-Al_2O_3

Oleg Alexeev,* Do-Woan Kim,* George W. Graham,† Mordecai Shelef,† and Bruce C. Gates*

*Department of Chemical Engineering and Materials Science, University of California, Davis, California 95616; and †Ford Research Laboratory, Ford Motor Co., Dearborn, Michigan 48121

Received December 18, 1998; accepted March 10, 1999

Samples of Pt on γ-Al_2O_3 were prepared by reduction in H_2 at 400°C of [$PtCl_2(PhCN)_2$], adsorbed intact from *n*-pentane solution onto γ-Al_2O_3 powder that had been partially dehydroxylated under vacuum at 400°C. The Pt dispersion was determined to be about 0.58 by standard methods, namely, chemisorption of hydrogen, of oxygen, and of CO, titration of chemisorbed oxygen with hydrogen, and extended X-ray absorption fine structure (EXAFS) spectroscopy. The supported Pt particles were resistant to sintering in the presence of O_2 at temperatures up to 400°C, as shown by chemisorption and EXAFS data, but the latter indicated that a combination of O_2 and H_2 treatments at 200–400°C led to changes in particle morphology. The samples were investigated by temperature-programmed desorption (TPD) of preadsorbed hydrogen; a TPD peak centered at 120°C represents hydrogen adsorbed on Pt and confirms the value of 0.58 for the dispersion. TPD of preadsorbed H_2 gave evidence of a second desorption peak, at 580°C, which was always accompanied by desorption of water at the same temperature; its presence was found to depend chiefly on the sample reduction temperature and evacuation time (it was absent when there was no Pt on the γ-Al_2O_3). The desorption of H_2 or D_2 that had been adsorbed on Pt/γ-Al_2O_3 reduced with D_2 or H_2, respectively, shows that hydrogen species desorbed at about 580°C originate from water (hydroxyl) species as a result of Pt-catalyzed decomposition.

INTRODUCTION

Although Pt/γ-Al_2O_3 is one of the best understood supported metal catalysts and chemisorption of H_2 one of the most useful methods for its characterization, there are still questions about high-temperature H_2 desorption and the surface structures involved. With the goal of understanding better the high-temperature desorption phenomena, we have investigated Pt/γ-Al_2O_3, characterizing it by standard chemisorption methods, infrared spectroscopy, extended X-ray absorption fine structure (EXAFS) spectroscopy, and temperature-programmed desorption (TPD).

EXPERIMENTAL

Reagents and Sample Preparation

Preparations and sample transfers were performed with air exclusion techniques, and gases [H_2 and CO (Matheson, UHP grade)] were purified by passage through traps containing reduced Cu/Al_2O_3 and zeolite to remove traces of O_2 and H_2O, respectively. Deuterium (Air Products and Chemicals, research grade) was used as supplied. The γ-Al_2O_3 support, with a BET surface area of 100 m^2/g determined by N_2 adsorption, was prepared as before (1) and evacuated at 400°C prior to use. *n*-Pentane solvent was purified by refluxing over Na/benzophenone ketyl and deoxygenated (1). Pt/γ-Al_2O_3 was prepared by slurrying [$PtCl_2(PhCN)_2$] (Strem) with γ-Al_2O_3 powder in *n*-pentane in amounts chosen to give a sample containing 1 wt% Pt; the pentane was removed by evacuation, ensuring complete uptake of the [$PtCl_2(PhCN)_2$] by the support. Before characterization, the dried sample was reduced with H_2 at 1 atm and 400°C.

Infrared Spectroscopy

A Mattson Cygnus 100 FTIR spectrometer was used to record spectra with a resolution of 2 cm^{-1}. The Pt/γ-Al_2O_3 powder was pressed in a gold wire mesh at 2000 lb/in^2 with a chromel–alumel thermocouple spot-welded to the center of the grid. The grid was placed in a high-vacuum infrared cell equipped with CaF_2 windows that allowed resistive heating of the sample in flowing H_2. Each sample was scanned 120 times, and the signal was averaged.

Chemisorption Measurements

An RXM-100 multifunctional catalyst testing and characterization system (Advanced Scientific Designs, Inc.) with a vacuum capability of 10^{-8} Torr was used for chemisorption measurements, as described earlier (2). The amount

0021-9517/99 $30.00

of hydrogen, oxygen, or CO irreversibly chemisorbed on the sample was measured as the difference between the total adsorption and the physical adsorption isotherms (two isotherms measured consecutively with 30 min evacuation between measurements). Errors in the determination of H/Pt, O/Pt, and CO/Pt values were as much as about ±10%.

Hydrogen (and Deuterium) TPD

The RXM-100 system has a high-vacuum capability (10^{-8} Torr) for TPD measurements. The sample handling and treatment procedures were essentially the same as those used for the chemisorption measurements (2); after reduction with H_2, the Pt/γ-Al_2O_3 sample was exposed to H_2 (or D_2) at room temperature and different pressures to give various Pt surface coverages. After evacuation at room temperature for 1 h to remove weakly adsorbed hydrogen, the sample was heated under vacuum as the temperature was ramped from 25 to 700°C at a rate of 10°C/min. Desorption of H_2 and H_2O (or D_2 and D_2O) was monitored with a quadrupole mass spectrometer (UTI model 100C). The pressure in the system was kept at approximately 4×10^{-5} Torr to prevent readsorption of desorbed hydrogen.

EXAFS Spectroscopy

EXAFS experiments were performed at X-ray beamline X-11A of the National Synchrotron Light Source (NSLS), Brookhaven National laboratory, Upton, NY. The storage ring energy was 2.5 GeV and the ring current 110–220 mA. The Pt/γ-Al_2O_3 sample was characterized after reduction at 400°C and after treatment with O_2 at different temperatures (100–400°C) followed by treatment with H_2 at 400°C. The sample mass was chosen to give an absorbance of about 2.5 at the Pt L_{III} absorption edge (11563.7 eV). Each sample was treated with H_2 at 400°C for 2 h in an EXAFS cell (3), cooled to room temperature in flowing H_2, evacuated to 10^{-5} Torr, and aligned in the X-ray beam. When an O_2 treatment was used, the cell was purged with He at the treatment temperature to remove traces of O_2, cooled to room temperature in flowing He, and treated with H_2. The EXAFS data were recorded in the transmission mode after the cell had been cooled to nearly liquid nitrogen temperature. The data were collected with a Si(111) double crystal monochromator that was detuned by 20% to minimize the effects of higher harmonics in the X-ray beam.

EXAFS REFERENCE DATA AND ANALYSIS

The EXAFS data were analyzed with the XDAP software (4) on the basis of experimentally determined reference files. The methods are essentially the same as those reported in Ref. (5). Data representing each sample are the average of six scans. Data characterizing the samples treated with H_2 at 400°C or with O_2 at different temperatures followed by treatment with H_2 at 400°C were analyzed as described below.

The raw data were Fourier-transformed with k^3 weighting over the range $2.69 < k < 15.80$ Å^{-1} (k is the wave vector) with no phase correction. The Fourier-transformed data were then inverse-transformed in the range $0.64 < r < 5.15$ Å (r is the distance from the Pt atom). The data analysis was done with 20 free parameters over the range $3.50 < k < 15.0$ Å^{-1} and $0.64 < r < 5.15$ Å. The statistically justified number of free parameters, n, was found to be 34, as estimated from the Nyquist theorem (6, 7), $n = (2\Delta k \Delta r/\pi) + 1$, where Δk and Δr are the k and r ranges, respectively, used in the fit. Other details are similar to those reported elsewhere (8).

RESULTS

Chemisorption and Metal Dispersion

The chemisorption data representing Pt/γ-Al_2O_3 after reduction at 400°C are summarized in Table 1. The numbers of H or O atoms or CO molecules adsorbed per total Pt atom were nearly the same. The amount of H_2 consumed during titration of preadsorbed oxygen (Table 2) on the sample reduced at 400°C was about three times the amount of O_2 adsorbed at room temperature, indicating that the hydrogen was consumed not only for reduction of adsorbed oxygen but also for formation of a monolayer of hydrogen on the Pt. Thus, the Pt dispersion (the fraction of Pt atoms exposed) calculated from the hydrogen titration data, assuming the stoichiometry of hydrogen titration equals 3, was found to be 0.57 (Table 2), in good agreement with values of H/Pt, O/Pt, and CO/Pt (Table 1). The corresponding average Pt particle diameter after reduction at 400°C is about 20 Å (9).

Treatment of Pt/γ-Al_2O_3 with O_2 at temperatures up to 400°C, followed by treatment with H_2 at 400°C, did not

TABLE 1

Influence of Treatment Conditions on Chemisorption Properties of the 1% Pt/γ-Al_2O_3 Samples Prepared from [$PtCl_2(PhCN)_2$] and Reduced in H_2 at 400°C

Temperature of treatment in O_2 (°C)[a]	Chemisorption at 25°C, atomic ratio[b]		
	H/Pt	CO/Pt	O/Pt
No treatment	0.58	0.57	0.58
200	0.60	0.64	0.59
300	0.55	0.57	0.60
400	0.57	0.55	0.55

[a] Samples were treated in 10% O_2 in He.

[b] For CO adsorption, the data represent the number of molecules of CO per Pt atom.

TABLE 2

Oxygen Chemisorption and Hydrogen Titration Data Characterizing 1% Pt/γ-Al_2O_3 Prepared from [$PtCl_2(PhCN)_2$] and Reduced in H_2 at 400°C

Temperature of treatment in O_2 (°C)[a]	Chemisorption at 200°C, O/Pt atomic ratio	Hydrogen titration[b]	Pt_s/Pt_t[c]
No treatment	0.73	1.70	0.57
200	0.76	1.74	0.58
300	0.76	1.80	0.60
400	0.76	1.69	0.56

[a] Samples were treated in 10% O_2 in He.

[b] Amount of hydrogen required for titration of chemisorbed oxygen was determined at 25°C, H/Pt atomic ratio.

[c] Dispersion expressed as the ratio of the number of surface Pt atoms to total number of Pt atoms in the sample, calculated from hydrogen titration data.

significantly change the Pt dispersion indicated by the chemisorption or hydrogen titration data. Thus, the sample was resistant to sintering, even in the presence of O_2, at temperatures up to 400°C; this result is important, as we are concerned with changes in the samples occurring at temperatures >400°C.

Infrared Spectra of CO Adsorbed on Pt/γ-Al_2O_3

When Pt/γ-Al_2O_3 reduced in H_2 at 400°C was exposed to 100 Torr of CO at room temperature, ν_{CO} bands appeared at 2078 and 1854 cm^{-1} (Fig. 1, Spectrum 1); these are assigned to linear and bridging CO adsorbed on metallic Pt, respectively (10–12). When the temperature of the evacuated sample was ramped to 400°C, the band assigned to the bridging CO disappeared first, and the terminal CO band declined in intensity and shifted to 2049 cm^{-1}; no ν_{CO} bands remained at 400°C (Fig. 1, Spectrum 8).

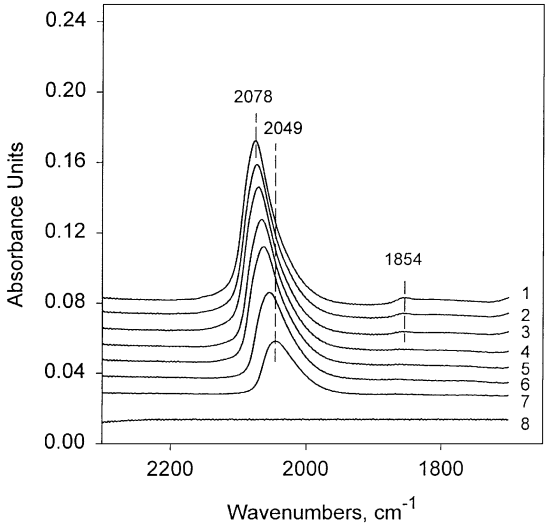

FIG. 1. Infrared spectra of CO adsorbed on sample prepared from [$PtCl_2(PhCN)_2$] on γ-Al_2O_3 and treated with H_2 at 400°C, following treatment in vacuum at the following temperatures (°C): (1) 25; (2) 50; (3) 72; (4) 115; (5) 150; (6) 240; (7) 350; (8) 400.

EXAFS Data

The results of the EXAFS data fitting are summarized in Table 3. Comparisons of the data and the fits are shown in Fig. 2. The estimated error bounds in Table 3 represent precisions determined from statistical analysis of the data, not accuracies. The estimated accuracies are as follows: Pt–Pt first-shell coordination number, ±15–20%; Pt–Pt distance, ±1%.

TPD Data

TPD profiles characterizing γ-Al_2O_3 that had been partially dehydroxylated under vacuum at different temperatures are shown in Fig. 3. Water ($m/e = 18$) was the only product observed, with the maximum desorption observed between 450 and 840°C, depending on the calcination temperature.

Figure 4 represents TPD profiles of hydrogen adsorbed at different surface coverages on Pt/γ-Al_2O_3 reduced at 400°C. Two major desorption peaks were observed, with maxima at 120 and 580°C. Quantification of the hydrogen desorbed at temperatures near 120°C (after saturation of the Pt surface with hydrogen) gave a H/Pt value of 0.58, in good agreement with the chemisorption data (Table 1). The hydrogen desorbed at temperatures near 580°C corresponds to a H/Pt value of 1.6. Thus, the total amount of hydrogen desorbed exceeds that which had been chemisorbed by addition of H_2. The intensity and shape of the high-temperature TPD peak depend on the evacuation time and reduction temperature. After long evacuation times (e.g., 10 h) at 400°C following reduction with H_2, a single peak was observed, with a maximum at 580°C (Figs. 4 and 5). But when the evacuation time was short (1 h), additional hydrogen desorption was observed (indicated by a shoulder at 500°C) (Fig. 5). When the reduction temperature was increased to 500°C, the high-temperature peak at about 580°C was no longer evident.

Besides hydrogen, water was always present in the TPD effluent (Figs. 6–8), its evolution being observed at temperatures just slightly higher than the highest pretreatment temperature (400°C). The total amount of water desorbed from Pt/γ-Al_2O_3 was about 2.7 times less than that desorbed from γ-Al_2O_3. Two maxima were typically distinguished in water TPD profile (at 580 (indicated by a shoulder) and 670°C (Figs. 6–8)). When Pt/γ-Al_2O_3 was reduced at 500°C, the water peak typically observed at 580°C was no longer evident.

To identify the different forms of desorbed hydrogen, experiments were done with (a) D_2 adsorbed on samples initially reduced with H_2 and (b) H_2 adsorbed on samples initially reduced with D_2. TPD results are illustrated in

TABLE 3

EXAFS Results at the Pt L_{III} Edge Characterizing the γ-Al_2O_3-Supported Sample Prepared from $[PtCl_2(PhCN)_2]$ and Treated in O_2 at Different Temperatures Followed by Treatment in H_2 at 400°C for 2 h[a]

Temperature of treatment in O_2 (°C)	Shell	Pt–Pt contribution				Pt–O_s contribution				Pt–O_l contribution			
		N	R (Å)	$10^3 \cdot \Delta\sigma^2$ (Å^2)	ΔE_0 (eV)	N	R (Å)	$10^3 \cdot \Delta\sigma^2$ (Å^2)	ΔE_0 (eV)	N	R (Å)	$10^3 \cdot \Delta\sigma^2$ (Å^2)	ΔE_0 (eV)
No treatment	first	8.8 ± 0.1	2.76 ± 0.01	5.8 ± 0.0	-3.9 ± 0.1	1.8 ± 0.1	2.11 ± 0.01	8.3 ± 1.8	-6.0 ± 0.1	0.7 ± 0.1	2.82 ± 0.01	-8.7 ± 0.1	11.3 ± 0.2
200	first	8.9 ± 0.1	2.76 ± 0.01	4.7 ± 0.1	-3.0 ± 0.1	0.9 ± 0.1	2.13 ± 0.01	9.4 ± 1.0	-6.0 ± 0.9	0.3 ± 0.1	2.84 ± 0.01	-10.0 ± 0.2	-1.2 ± 0.3
300	first	8.8 ± 0.1	2.76 ± 0.01	3.9 ± 0.1	-3.4 ± 0.1	0.7 ± 0.1	2.16 ± 0.01	6.9 ± 0.7	-10.0 ± 0.5	0.3 ± 0.1	2.83 ± 0.01	-10.0 ± 0.2	0.3 ± 0.2
400	first	8.9 ± 0.1	2.76 ± 0.01	4.1 ± 0.1	-3.6 ± 0.1	0.9 ± 0.1	2.16 ± 0.01	10.0 ± 0.9	-6.9 ± 0.8	0.2 ± 0.1	2.85 ± 0.01	-10.0 ± 0.2	-3.6 ± 0.3
No treatment	second	4.1 ± 0.1	3.90 ± 0.01	5.0 ± 0.2	0.0 ± 0.1	—	—	—	—	—	—	—	—
200	second	3.9 ± 0.1	3.90 ± 0.01	5.0 ± 0.2	0.0 ± 0.2	—	—	—	—	—	—	—	—
300	second	2.9 ± 0.1	3.90 ± 0.01	3.5 ± 0.2	1.0 ± 0.2	—	—	—	—	—	—	—	—
400	second	2.5 ± 0.1	3.90 ± 0.01	2.5 ± 0.2	-1.2 ± 0.2	—	—	—	—	—	—	—	—
No treatment	third	4.4 ± 0.1	4.80 ± 0.01	1.0 ± 0.1	-5.5 ± 0.1	—	—	—	—	—	—	—	—
200	third	5.0 ± 0.1	4.80 ± 0.01	1.5 ± 0.1	-6.0 ± 0.1	—	—	—	—	—	—	—	—
300	third	7.2 ± 0.2	4.80 ± 0.01	2.8 ± 0.1	-6.0 ± 0.1	—	—	—	—	—	—	—	—
400	third	8.2 ± 0.2	4.80 ± 0.01	3.2 ± 0.1	-5.5 ± 0.1	—	—	—	—	—	—	—	—

[a] Notation: N, coordination number; R, distance between absorber and backscatterer atoms; $\Delta\sigma^2$, Debye–Waller factor; ΔE_0, inner potential correction; the subscripts s and l refer to short and long, respectively.

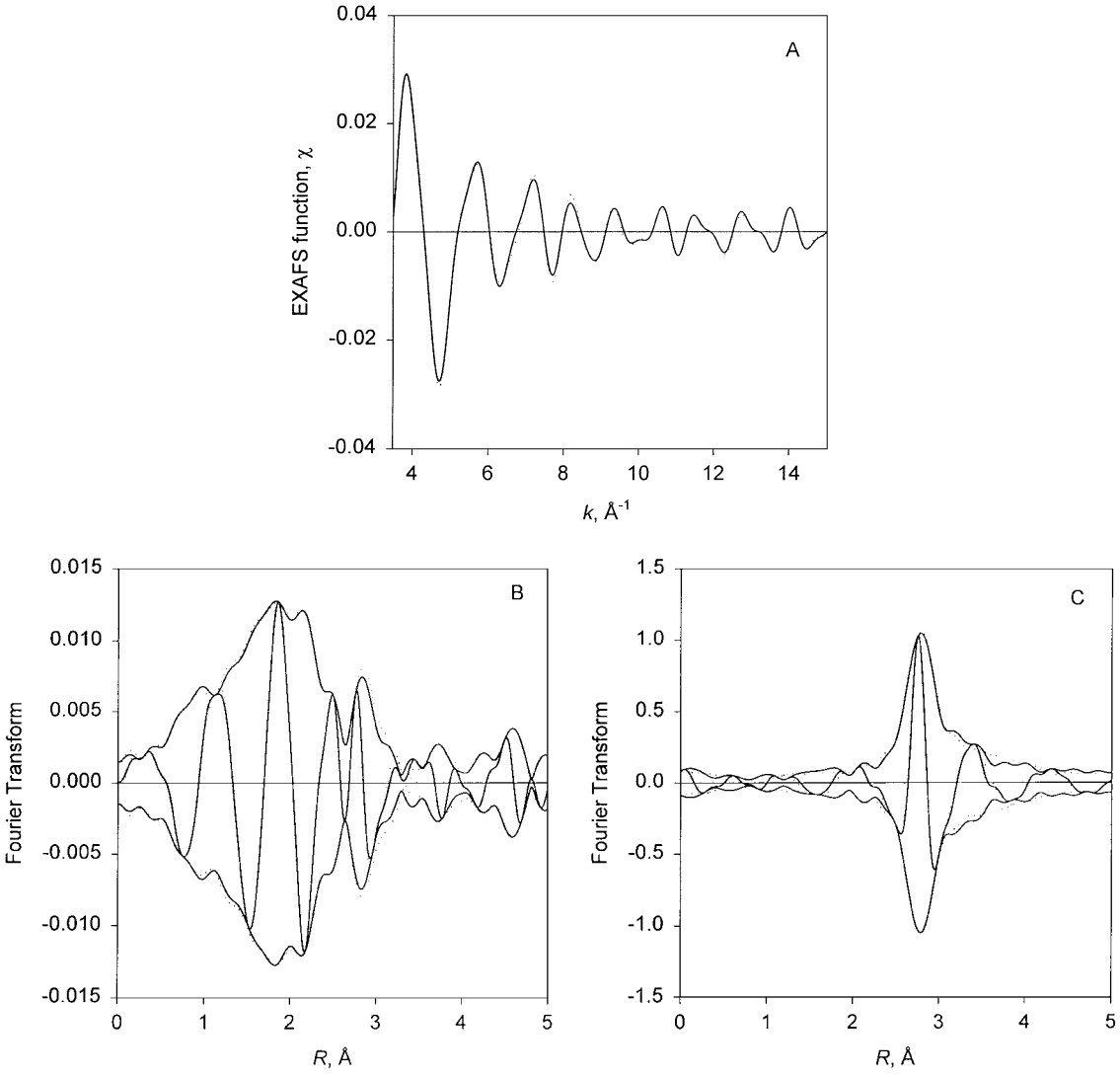

FIG. 2. Results of analysis of Pt L_{III} edge EXAFS data obtained with the best calculated coordination parameters characterizing the Pt/γ-Al_2O_3 sample prepared from $[PtCl_2(PhCN)_2]$ precursor following treatment in H_2 at 400°C: (A) experimental EXAFS function (solid line) and sum of the calculated Pt–Pt (first shell, second shell, and third shell) + Pt–$O_{support}$ (Pt–O_s and Pt–O_l) contributions (dotted line); (B) imaginary part and magnitude of uncorrected Fourier transform (k^0 weighted, $\Delta k = 3.50$–15.00 Å^{-1}) of experimental EXAFS (solid line) and sum of the calculated Pt–Pt (first shell, second shell, and third shell) + Pt–$O_{support}$ (Pt–O_s and Pt–O_l) contributions (dotted line); (C) imaginary part and magnitude of phase- and amplitude-corrected Fourier transform (k^1 weighted, $\Delta k = 3.50$–15.00 Å^{-1}) of raw data minus the calculated Pt–Pt (second shell and third shell) and Pt–$O_{support}$ (Pt–O_s and Pt–O_l) contributions (solid line) and calculated Pt–Pt first-shell contribution (dotted line); (D) imaginary part and magnitude of phase- and amplitude-corrected Fourier transform (k^3 weighted, $\Delta k = 3.50$–15.00 Å^{-1}) of raw data minus calculated Pt–Pt (second shell and third shell) and Pt–$O_{support}$ (Pt–O_s and Pt–O_l) contributions (solid line) and calculated Pt–Pt first-shell contribution (dotted line); (E) imaginary part and magnitude of phase- and amplitude-corrected Fourier transform (k^3 weighted, $\Delta k = 3.50$–15.00 Å^{-1}) of raw data minus calculated Pt–Pt (first shell and third shell) and Pt–$O_{support}$ (Pt–O_s and Pt–O_l) contributions (solid line) and calculated Pt–Pt second-shell contribution (dotted line); (F) imaginary part and magnitude of phase- and amplitude-corrected Fourier transform (k^3 weighted, $\Delta k = 3.50$–15.00 Å^{-1}) of raw data minus calculated Pt–Pt (first shell and second shell) and Pt–$O_{support}$ (Pt–O_s and Pt–O_l) contributions (solid line) and calculated Pt–Pt third-shell contribution (dotted line); (G) residual spectrum illustrating Pt–$O_{support}$ contributions: imaginary part and magnitude of phase-corrected Fourier transform (k^0 weighted, $\Delta k = 3.50$–15.00 Å^{-1}) of raw data minus calculated Pt–Pt contribution (solid line) and calculated Pt–$O_{support}$ (Pt–O_s and Pt–O_l) contribution (dotted line).

Fig. 6A for Pt/γ-Al_2O_3 reduced with H_2 at 400°C, evacuated at 400°C for 10 h, and then treated with D_2 to give a 75% Pt surface coverage (as determined by chemisorption data).

In the low-temperature region, several different desorbed hydrogen species were observed; besides the peak representing desorbed D_2 (with a maximum at 124°C), peaks indicating HD and H_2 were observed, with maxima at 169 and 217°C, respectively. In addition, several hydrogen species were observed in the high-temperature region (Fig. 6A), each with a desorption peak maximum at 580°C,

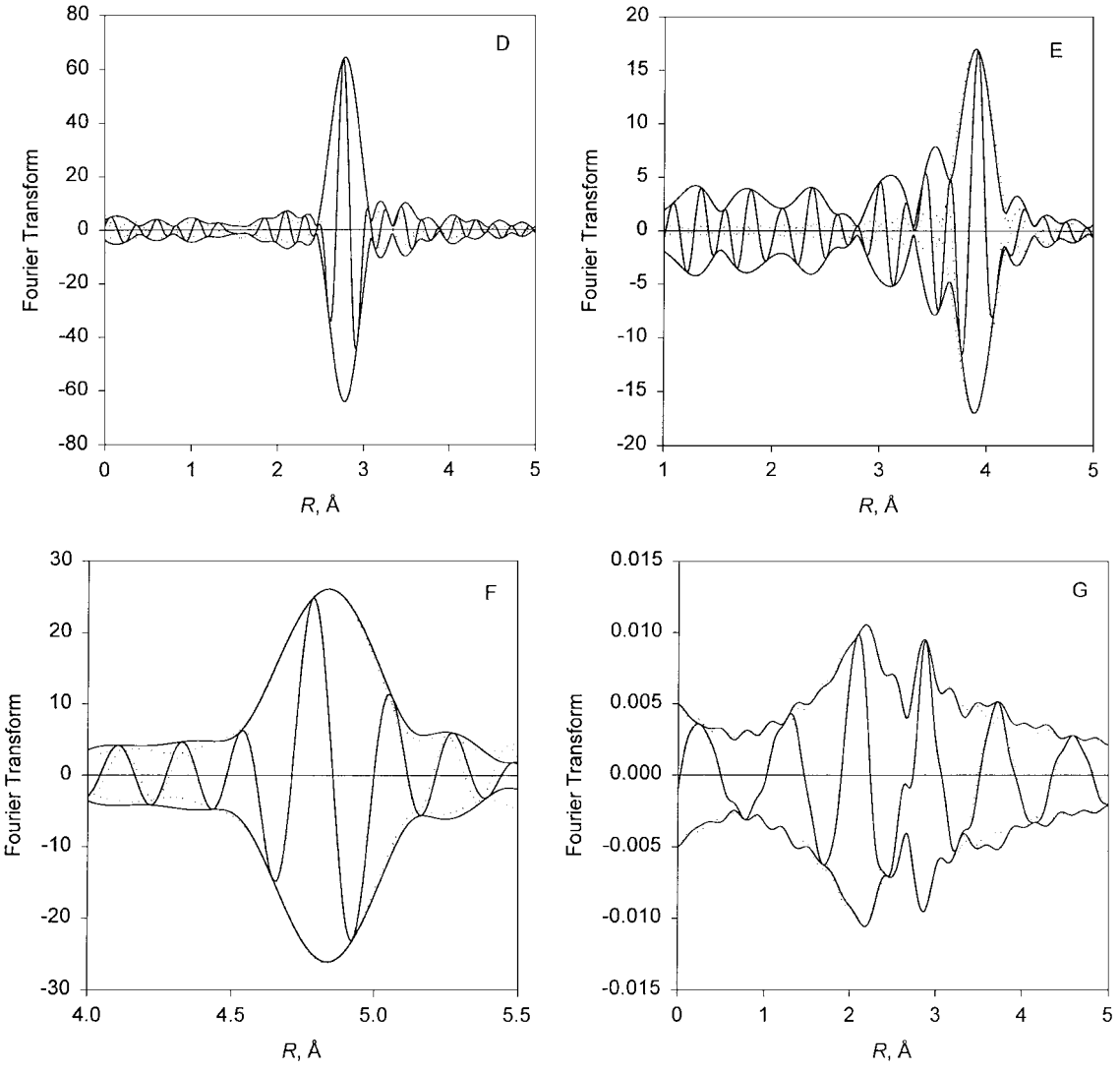

FIG. 2—*Continued*

and the intensities of the desorption peaks decreased in the order $H_2 > HD > D_2$. Water was also observed in the high-temperature region (Fig. 6B), with two maxima, at 580 (indicated by a shoulder) and 670°C. The former temperature matches that observed for the hydrogen species. The intensities of the peaks indicating water species declined in the order $H_2O > HDO > D_2O$ (Fig. 6B), and the trend matches that observed for the respective hydrogen species ($H_2 > HD > D_2$) desorbed in the same temperature range.

Profiles are shown in Figs. 7A and 7B for hydrogen and water desorbed from the sample reduced with H_2 at 400°C for 2 h, exposed to 780 Torr of D_2 for 1 h, and then evacuated at 400°C for 10 h. This sample is characterized by a lack of desorption in the low-temperature region, as expected, and by desorption of both hydrogen and water in the high-temperature region. The results are similar to those characterizing the several samples mentioned above on which H_2 and D_2 had been preadsorbed insofar as the desorption maxima were observed at 580°C for all the forms of hydrogen (Fig. 7A).

This temperature matches one of the two temperatures representing peaks in the water TPD profiles (Fig. 7B). The amount of water desorbed as HDO exceeded that desorbed as H_2O or D_2O. The peaks corresponding to the latter two species were about equal in intensity, which suggests that about 50% of the OH groups were exchanged during the D_2 treatment. A similar pattern was observed for the desorbed hydrogen species; the most intense peak was observed for HD, and the intensities of the H_2 and D_2 peaks were about equal to each other.

When H_2 was adsorbed on the sample pretreated with D_2, most of the preadsorbed hydrogen was desorbed as H_2, with the peak centered at about 151°C (Fig. 8A), but HD and D_2 were also observed, with the peaks centered at about 212

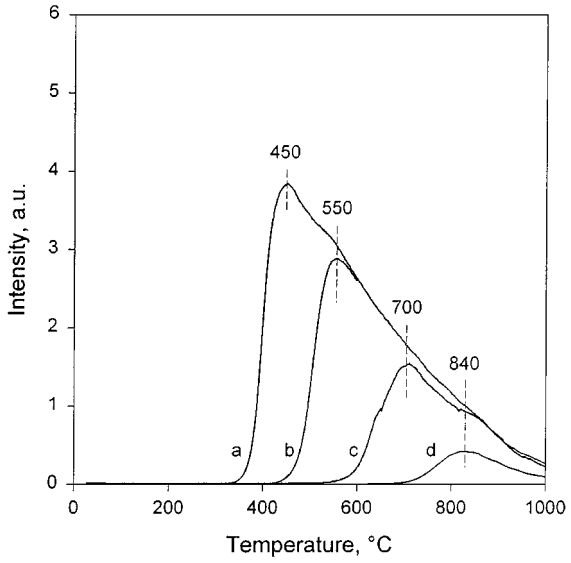

FIG. 3. TPD profiles of H_2O from bare γ-Al_2O_3 that had been calcined at different temperatures (°C): (a) 300; (b) 400; (c) 500; and (d) 600.

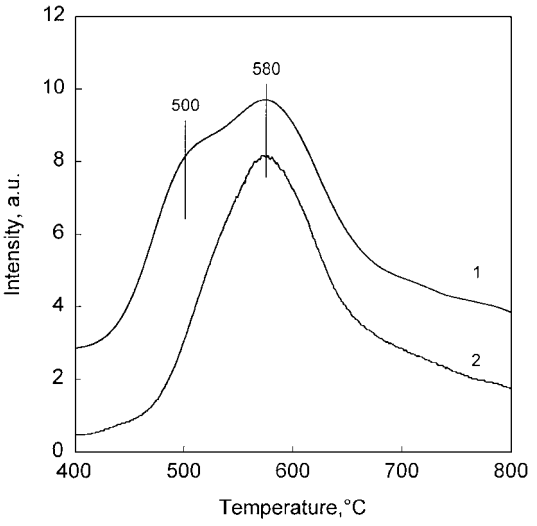

FIG. 5. TPD in the high-temperature region of hydrogen preadsorbed at monolayer coverage on the sample prepared from $[PtCl_2(PhCN)_2]$ on γ-Al_2O_3 and treated with H_2 at 400°C: (1) sample evacuated for 1 h after reduction; (2) sample evacuated for 10 h after reduction.

and 240°C, respectively. In the high-temperature region, three hydrogen species were distinguished, with TPD maxima for each at 580°C and intensities that declined in the order $HD > H_2 > D_2$ (Fig. 8A). Along with the hydrogen species, water species were observed as well (Fig. 8B), with peaks centered at 580 (indicated by a shoulder) and 670°C; the former matches that observed for the hydrogen species (Fig. 8A). The intensities of the water peaks declined in the order $HDO > H_2O > D_2O$; again, the observed trend matches that observed for hydrogen species desorbed in the same temperature region (Fig. 8A).

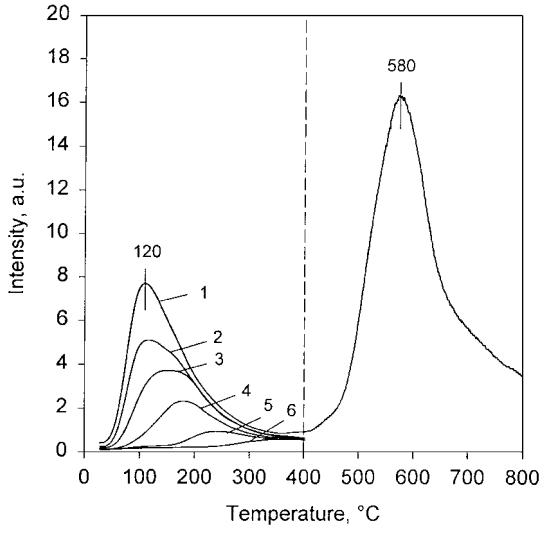

FIG. 4. TPD profiles of hydrogen preadsorbed at different surface coverages on the sample prepared from $[PtCl_2(PhCN)_2]$ on γ-Al_2O_3 and treated with H_2 at 400°C: (1) monolayer (100%) Pt surface coverage; (2) 75% Pt surface coverage; (3) 50% Pt surface coverage; (4) 35% Pt surface coverage; (5) 25% Pt surface coverage; and (6) 10% Pt surface coverage.

DISCUSSION

Consistency of Data Determining Pt Dispersion

The good agreement of the Pt dispersions determined by the chemisorption data (Table 1) verifies the assumption that each surface Pt atom combines with one H atom, O atom, or CO molecule; the CO data agree with the infrared spectra (Fig. 1) showing that CO adsorption was mainly terminal. The chemisorption data also confirm that the stoichiometry of hydrogen titration equals 3 (Tables 1 and 2), independent of the average Pt particle size or pretreatment conditions (13), so that each O atom reacts with two hydrogen atoms to give water, with the remaining hydrogen being adsorbed on Pt (14). The data also imply that the Pt particles were not completely oxidized and the sample was virtually free of surface carbon residues. Thus, the data show that the Pt/γ-Al_2O_3 sample is relatively simple and well defined and therefore a good candidate for the high-temperature investigation reported here.

The EXAFS data provide a complementary basis for estimating the Pt dispersion. Interpretation of these data must rely on some assumed relationship between the observed metal–metal coordination number and average metal particle size, which is a function of the particle geometry (15–17). When the particle diameters are greater than about 10 Å, the choice of a geometric model for the particles is important (18), which may explain in part why only some estimates of metal dispersion based on EXAFS data are

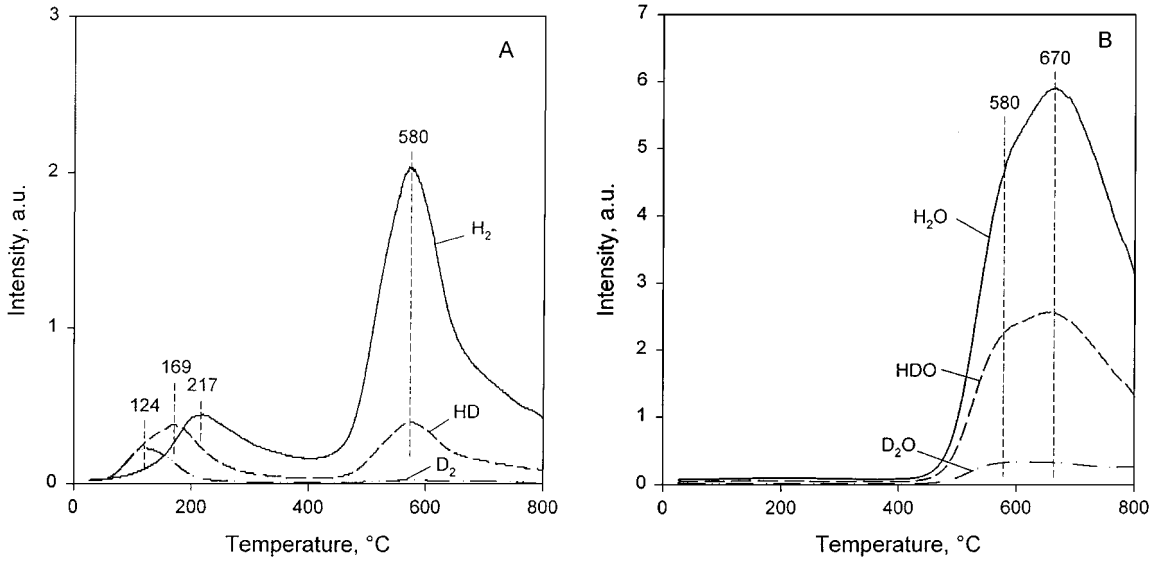

FIG. 6. TPD profiles of various (A) hydrogen and (B) water species formed after adsorption of D_2 at 75% of monolayer Pt surface coverage on Pt/γ-Al_2O_3 initially reduced with H_2 at 400°C for 2 h and evacuated at 400°C for 10 h.

in good agreement with estimates based on other techniques, including hydrogen chemisorption (5), transmission electron microscopy, or X-ray diffraction line broadening (5, 19, 20).

One expects relationships between the metal–metal first-shell coordination number (and also the higher-shell coordination numbers) and the number of metal atoms in a particle. Because of limitations of the models and the fact that the EXAFS data determine only average structural information, the metal dispersion estimated on the basis of a first-shell coordination number may be different from that estimated on the basis of higher-shell coordination numbers. Such differences might also be explained in part by the fact that the structural parameters determined from higher-shell EXAFS data are relatively inaccurate because of overlapping of shells and multiple scattering phenomena. The differences may be as much as the 30–65% observed for Pt/NaY zeolite (5).

Consequently, we have relied on first-shell and not higher-shell EXAFS data to estimate the Pt dispersion. The

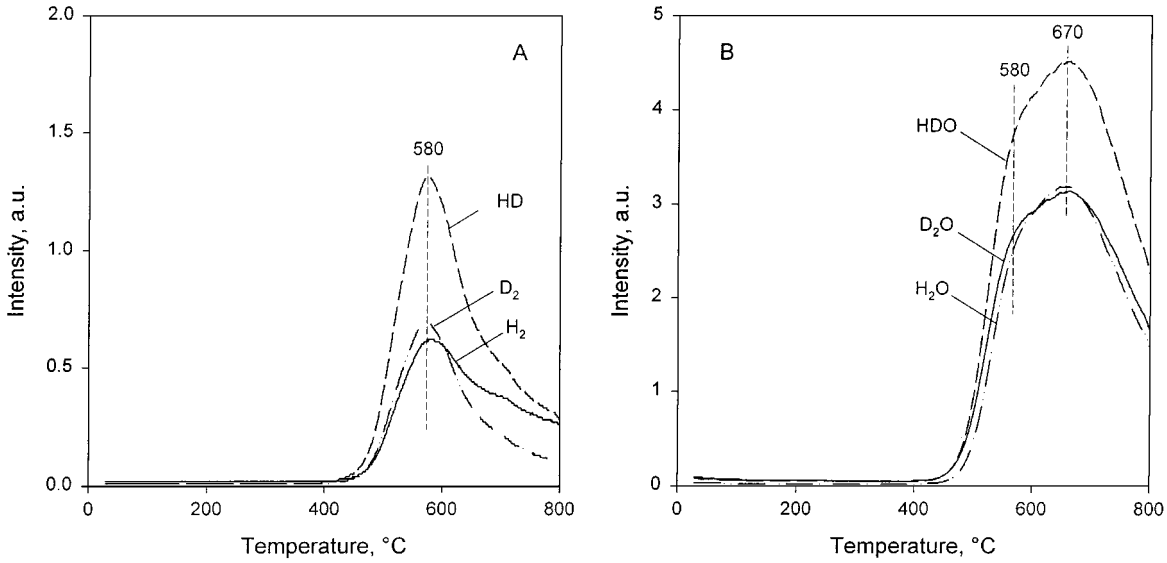

FIG. 7. TPD profiles of various (A) hydrogen and (B) water species evolving from Pt/γ-Al_2O_3 that had been first reduced with H_2 at 400°C for 2 h then exposed to 780 Torr of D_2 for 1 h and evacuated at 400°C for 10 h.

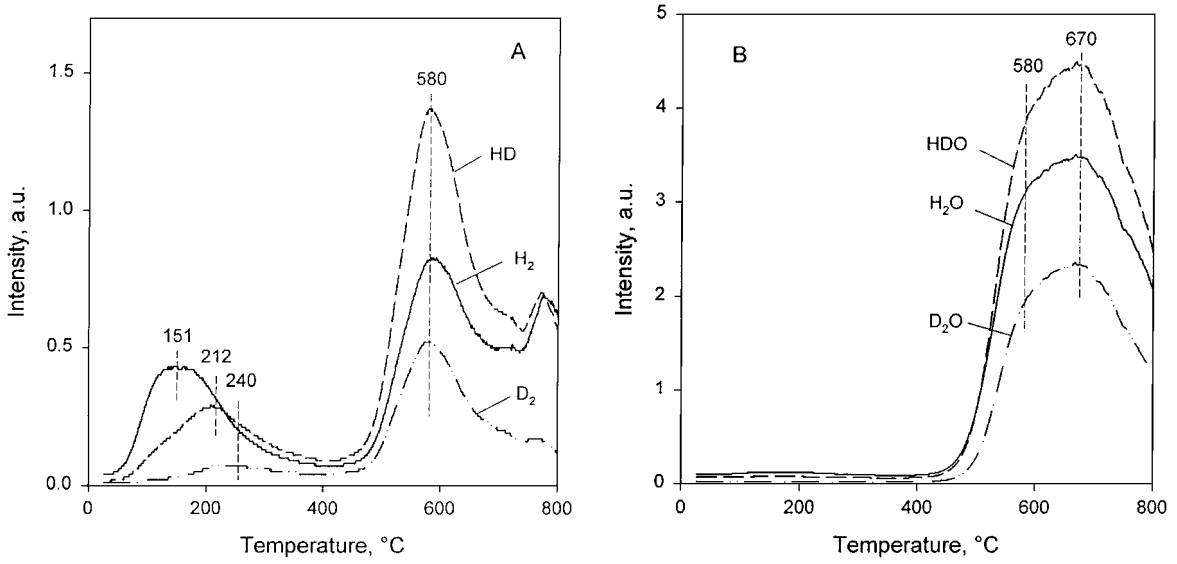

FIG. 8. TPD profiles of various (A) hydrogen and (B) water species formed after adsorption of H_2 at 75% of Pt monolayer surface coverage on Pt/γ-Al_2O_3 that had been first reduced with H_2 at 400°C for 2 h then exposed to 780 Torr of D_2 for 1 h and evacuated at 400°C for 10 h.

estimate is based on the model of Kip *et al.* (21), whereby the fcc metal structure and an epitaxial arrangement of metal atoms on the (111) surface of γ-Al_2O_3 are assumed. This model is not based on any assumed particle geometry; rather, the shape of the average metal particle was calculated as a function of the relative magnitude of the metal–metal and metal–support interaction energy by minimizing the total energy; the shape of a metal particle with $n+1$ atoms was estimated from that of the particle with n atoms by putting the extra metal atom in the position of minimum energy (21). The results for Pt/γ-Al_2O_3 after reduction with H_2 at 400°C give a Pt dispersion (0.58) in good agreement with the values determined by the chemisorption data (Tables 2 and 4); the agreement extends to the sample treated with O_2 and H_2 under different conditions (Table 4). Thus, the data provide the first thorough comparison of

TABLE 4

Comparison of Pt Dispersion Determined from Chemisorption and EXAFS Data for Pt/γ-Al_2O_3 Samples Treated under Different Conditions

Treatment conditions	Chemisorption		EXAFS			
	Pt_s/Pt_t[a]	Average particle size, Å[b]	N_{Pt-Pt}	Normalized diameter (in metal atom diameters)	Average particle size, Å[c]	Pt_s/Pt_t[c]
H_2 at 400°C	0.57	19.9	8.8	7.9	21.8	0.58
O_2 at 200°C followed by H_2 at 400°C	0.58	19.5	8.9	8.2	22.6	0.57
O_2 at 300°C followed by H_2 at 400°C	0.60	18.9	8.8	7.9	21.8	0.58
O_2 at 400°C followed by H_2 at 400°C	0.56	20.2	8.9	8.2	22.6	0.57

[a] Dispersion (fraction of surface atoms exposed) calculated from hydrogen titration data.

[b] Average particle diameter d_{Pt} was calculated assuming that the Pt particles are spherical, according to the equation $d_{Pt} = 11.32/(Pt_s/Pt_t)$.

[c] Pt particle size and dispersion were estimated from first-shell Pt–Pt coordination numbers using the model reported by Kip *et al.* (21).

Pt dispersions estimated from EXAFS and chemisorption data for Pt/γ-Al_2O_3 samples treated under indentical conditions. EXAFS spectroscopy determines the Pt dispersion accurately.

Influence of O_2 Treatment on Pt Dispersion

The data demonstrate the thermal stability of the samples treated in H_2 at temperatures up to 400°C, consistent with earlier data (22). The chemisorption and oxygen titration data (Tables 1 and 2), in agreement with the EXAFS data (Tables 3 and 4), show that the oxidation–reduction treatments at 200–400°C did not significantly influence the Pt dispersion. However, similar oxygen–hydrogen treatments at temperatures >400°C have been observed to cause substantial sintering of supported Pt particles (16).

EXAFS Evidence of the Metal-Support Interface and Pt Particle Morphology

The metal–oxygen contributions indicated by the EXAFS data (Table 3) show that treatment of the sample with O_2 at different temperatures followed by treatment with H_2 at 400°C did not substantially influence the interaction between Pt and the support (Table 3), but it did lead to changes in the Pt particle morphology. When Pt/γ-Al_2O_3 was reduced at 400°C, Pt–Pt first-, second-, and third-shell contributions were observed, indicating the formation of relatively large Pt particles. The combination of O_2 and H_2 treatments did not significantly influence the Pt–Pt distances of the three coordination shells or the Pt–Pt first-shell coordination number. However, the Debye–Waller factor characterizing the thermal disorder in the first Pt shell decreased with increasing temperature of O_2 treatment (Table 3), and major changes were observed in the EXAFS parameters for the second and the third coordination shells (Table 3). The data show that the combination of O_2 and H_2 treatments caused the Pt particles to become raft-like. The changes in particle morphology do not substantially affect the EXAFS evidence of the metal–support interface because the Pt particles were relatively large and the metal–support contributions only a small part of the overall EXAFS signal.

TPD of Hydrogen from Pt/γ-Al_2O_3

The low-temperature (<400°C) and high-temperature (>400°C) regions are distinct in typical TPD spectra of hydrogen from Pt/γ-Al_2O_3, as shown in the literature (23–27) and confirmed by the data presented here. The position of the TPD peak maximum and the quantity of H_2 desorbed in the low-temperature region are functions of the surface coverage by hydrogen (Fig. 4), which implies that there were hydrogen species differing from each other in coordination and strength of interaction with the surface. The data are thus similar to those characterizing desorption of H_2 from single-crystal Pt (28, 29) or supported Pt crystallites (25, 30) and suggest a second-order desorption from Pt with a rate-limiting recombination of H atoms (31).

Because the amount of hydrogen desorbed in the low-temperature region from Pt/γ-Al_2O_3 reduced at 400°C corresponds to a H/Pt ratio of 0.58, in agreement with the Pt dispersion determined by the chemisorption and EXAFS data, the peak observed in the low-temperature region is assigned simply to desorption of hydrogen chemisorbed on Pt (31).

Hydrogen Species Desorbed at High Temperatures

The H/Pt ratio (1.6) corresponding to hydrogen desorbed at temperatures >400°C exceeds that corresponding to the low-temperature desorption from Pt (0.58) and is independent of the Pt coverage by hydrogen. Thus, the hydrogen desorbed at these high temperatures was not simply hydrogen chemisorbed on Pt.

High-temperature hydrogen desorption peaks have been observed before for Pt/γ-Al_2O_3 (23, 24, 33) and Pt/zeolites (23), and possible explanations for them include oxidation of Pt by support protons (34, 35), strong chemisorption of hydrogen on Pt (36–38), spillover of hydrogen (39–41), formation of subsurface hydrogen (27), and adsorption of hydrogen on Pt–Al alloy (42, 43). These explanations have been assessed by Miller *et al.* (23), who ruled most of them out, except for spillover of hydrogen.

Although the amount of hydrogen desorbed from our samples at temperatures >400°C was about the same as that observed earlier for Pt/γ-Al_2O_3 and Pt/zeolite (23, 24, 33), our data are not accounted for by the explanations cited above. The data show that the shape and intensity of the peak representing hydrogen desorbing at temperatures >400°C depend on the evacuation time, reduction temperature, and presence of Pt in the sample. When bare γ-Al_2O_3, which had been calcined at various temperatures, was examined by TPD (Fig. 3), only water (and no hydrogen) was observed in the profiles. Since molecularly adsorbed water can be removed from γ-Al_2O_3 by evacuation at temperatures <300°C, we infer that the water observed in the TPD profiles at temperatures >400°C resulted from condensation of surface hydroxyl groups. The water TPD profiles (Fig. 3) are consistent with the inference that various hydroxyl species were present on the γ-Al_2O_3 surface, depending on the calcination temperature (44).

The following observations—(a) evolution of hydrogen in the high-temperature region occurred only when Pt was present in the sample and (b) a hydrogen peak in the high-temperature region was always accompanied by a water peak at the same temperature (580°C)—show that the hydrogen observed in the high-temperature region is associated only with those hydroxyl groups that are involved in desorption to give the peak at 580°C. TPD data obtained after reduction of Pt/γ-Al_2O_3 at 500°C support this

inference: whereas a water desorption peak was observed near 670°C (data not shown), no hydrogen peak was observed in the high-temperature region.

After Pt/γ-Al_2O_3 had been reduced with H_2 at 400°C, exposed to D_2, and then evacuated at the reduction temperature, three peaks, representing HD, H_2, and D_2 were observed (Fig. 7A), with maxima at the same temperature (580°C). The data imply that exchange occurred between D_2 and surface OH groups, presumably after D_2 dissociated on the Pt surface. This reaction is known to occur on bare γ-Al_2O_3 at temperatures >150°C (44) and in the presence of noble metal even at room temperature (45). Peaks were also observed for HDO, H_2O, and D_2O (Fig. 7B). Most important, the intensities of the hydrogen species decline in the same order as those observed for the corresponding water species. These data are consistent with earlier observations showing that exposure of Pt/γ-Al_2O_3 to traces of water results in hydrogen desorption in the high-temperature region even when no hydrogen was preadsorbed (25).

Thus, the data demonstrate that surface hydroxyl groups, which combine during thermal desorption (resulting in the formation of water) are the source of the hydrogen species—the formation of hydrogen at temperatures >400°C is the result of decomposition of surface hydroxyl groups (or water formed from them), and this must be catalyzed by the Pt.

Experiments carried out with H_2 adsorbed on samples reduced with D_2 (and with adsorption of D_2 on samples reduced with H_2) confirm this conclusion. In both cases, a variety of hydrogen species (H_2, HD, D_2) were observed during TPD in the low-temperature region (Figs. 6A and 8A), which are explained by exchange between adsorbed D (or H) atoms and H (or D) atoms of surface hydroxyl groups. Desorption of H_2 or D_2 was always observed at lower temperatures than desorption of partially exchanged (HD) or completely exchanged (D_2 or H_2) species (Figs. 6A and 8A). These results show that a relatively high degree of exchange was observed for the adsorbed H or D species that are strongly bonded to the Pt surface and located presumably at adsorption sites of high coordination.

When H_2 was adsorbed on the sample that had been reduced with D_2, most of the preadsorbed hydrogen was desorbed as H_2. On the other hand, when D_2 was adsorbed on the sample that had been reduced with H_2, the larger portion of desorbed species was H_2 and HD. The implication of these results is that at room temperature adsorbed deuterium atoms replace hydrogen atoms of surface OH groups more readily than adsorbed hydrogen atoms replace deuterium of surface OD groups.

Thus, the composition of species desorbing from the Pt surface at low temperatures is influenced by the chemical reactions that take place between hydroxyl groups and the adsorbate formed from H_2 or D_2. But the isotope exchange between adsorbate hydrogen and surface hydroxyl groups primarily defines the composition of the species desorbing at high temperatures. For example, when the sample had been reduced with H_2 so that all the hydroxyl groups were OH, and D_2 was adsorbed, most of the hydroxyl groups were still present as OH, and only a small fraction were present as OD as a result of the isotopic exchange, as shown by the intensities of the water species (H_2O, HDO, D_2O) observed during TPD in the high-temperature region (Fig. 6B).

Consistent with the above-stated conclusions, the experiments carried out with H_2 (or D_2) adsorbed on the sample reduced with D_2 (or H_2) indicate that the hydrogen species desorbing in the high-temperature range (Figs. 6A and 8A) are also determined primarily by the hydroxyl species on the γ-Al_2O_3, which confirms that the hydrogen species desorbed at these temperatures originate from hydroxyl groups. This idea is related to that of Ehwald and Leibnitz (25), who assumed that surface OH groups could oxidize the reduced centers (impurities) of γ-Al_2O_3, releasing hydrogen.

The TPD results do not provide evidence of the oxygen species formed as a result of the hydroxyl group decomposition, because no oxygen was detected in the TPD effluent. However, the following suggestion is made on the basis of the TPD data.

As 400°C was the highest temperature used to treat γ-Al_2O_3 or Pt/γ-Al_2O_3 during sample preparation or reduction, it is reasonable to expect that heating of the sample to higher temperatures (as was done in the TPD experiments) would have resulted first in structural changes of the γ-Al_2O_3—changes in the degree of dehydroxylation and perhaps the surface area. According to the model of Knözinger and Ratnasamy (44), a regular surface lattice of γ-Al_2O_3 can be maintained up to 67% dehydroxylation, which corresponds to a degassing temperature of about 500°C. The remaining adjacent OH groups can condense to eliminate water only by creation of defects consisting of coordinatively unsaturated Al^{3+} ions and oxygen vacancies. Because the hydrogen evolution (catalyzed by Pt) takes place in the same temperature range as the formation of surface defects resulting from dehydroxylation, we suggest that oxygen species formed as a result of this process could be stabilized by these defect sites (oxygen vacancies).

CONCLUSIONS

Pt/γ-Al_2O_3 was formed with a dispersion of near 0.58, as near shown by chemisorption of hydrogen, oxygen, and CO; hydrogen titration of chemisorbed oxygen; TPD of chemisorbed hydrogen at temperatures up to 400°C; and EXAFS spectroscopy. The Pt particles were resistant to sintering in the presence of O_2 at temperatures up to 400°C, as shown by the chemisorption and EXAFS data. The EXAFS data show that the Pt particles became raft-like as a result of

combination of oxygen-hydrogen treatments at 200–400°C. The high-temperature (>400°C) hydrogen TPD profiles were independent of the surface coverage by hydrogen; the high-temperature (580°C) peak was always accompanied by desorption of water at the same temperature, being dependent on the reduction temperature, evacuation time, and the presence of Pt on the γ-Al_2O_3. The data characterizing the desorption of H_2 (or D_2) that had been adsorbed on the Pt/γ-Al_2O_3 reduced with D_2 (or H_2) show that the hydrogen species desorbed in the high-temperature range originate from hydroxyl groups desorbed in the same temperature range as a result of their decomposition catalyzed by Pt.

ACKNOWLEDGMENTS

This research was supported by the National Science Foundation (GOALI Grant CTS-9529455) and by Ford Motor Co. We acknowledge beam time and the support of the U.S. Department of Energy, Division of Materials Sciences, under Contract DE-FG05-89ER45384, for its role in the operation and development of beam line X-11A at the National Synchrotron Light Source. The NSLS is supported by the Department of Energy, Division of Materials Sciences and Division of Chemical Sciences, under Contract DE-AC02-76CH00016. We are grateful to the staff of beam line X-11A for their assistance. The EXAFS data were analyzed with XDAP (4).

REFERENCES

1. Alexeev, O., Panjabi, G., and Gates, B. C., *J. Catal.* **173**, 196 (1998).
2. Alexeev, O., Shelef, M., and Gates, B. C., *J. Catal.* **164**, 1 (1996).
3. Jentoft, R. E., Deutsch, S. E., and Gates, B. C., *Rev. Sci. Instrum.* **67**, 2111 (1996).
4. Vaarkamp, M., Linders, J. C., and Koningsberger, D. C., *Physica B* **208&209**, 159 (1995).
5. Pandya, K. I., Heald, S. M., Hriljac, J. A., Petrakis, L., and Fraissard, J., *J. Phys. Chem.* **100**, 5070 (1996).
6. Brigham, O. E., "The Fast Fourier Transform," Prentice-Hall, Englewood Cliffs, NJ, 1974.
7. Stern, E. A., *Phys. Rev. B* **48**, 9825 (1993).
8. Alexeev, O., and Gates, B. C., *J. Catal.* **176**, 310 (1998).
9. Anderson, J. R., "Structure of Metallic Catalysts," Academic Press, London, 1975.
10. Little, L. H., "Infrared Spectra of Adsorbed Species," Academic Press, London, 1966.
11. Primet, M., Elazhar, M., Frety, R., and Guenin, M., *Appl. Catal.* **59**, 153 (1990).
12. Hayden, B. E., and Bradshaw, A. M., *Surf. Sci.* **125**, 787 (1983).
13. Prasad, J., Murthy, K. R., and Menon, P. G., *J. Catal.* **52**, 515 (1978).
14. Benson, J. E., and Boudart, M., *J. Catal.* **4**, 704 (1965).
15. Greegor, R. B., and Lytle, F. W., *J. Catal.* **63**, 476 (1980).
16. Borgina, A., Normand, F. L., Garetto, T., Apesteguia, C. R., and Moraweck, B., *Catal. Lett.* **13**, 175 (1992).
17. Benfield, R. E., *J. Chem. Soc. Faraday Trans.* **88**, 1107 (1992).
18. Díaz-Moreno, S., Koningsberger, D. C., and Muñoz-Páez, A., *Nucl. Instrum. Meth. Phys. Res. B* **133**, 15 (1997).
19. Shpiro, E. S., Joyner, R. W., Minachev, K. M., and Pudney, P. D. A., *J. Catal.* **127**, 366 (1991).
20. Clausen, B. S., Gråbæk, L., Topsøe, H., Hansen, L. B., Stoltze, P., Nørskov, J. K., and Nielsen, O. H., *J. Catal.* **141**, 368 (1993).
21. Kip, B. J., Duivenvoorden, F. B. M., Koningsberger, D. C., and Prins, R., *J. Catal.* **105**, 26 (1987).
22. Koningsberger, D. C., and Vaarkamp, M., *Physica B* **208&209**, 633 (1995).
23. Miller, J. T., Meyers, B. L., Modica, F. S., Lane, G. S., Vaarkamp, M., and Koningsberger, D. C., *J. Catal.* **143**, 395 (1993).
24. Miller, J. T., Meyers, B. L., Barr, M. K., Modica, F. S., and Koningsberger, D. C., *J. Catal.* **159**, 41 (1996).
25. Ehwald, H., and Leibnitz, U., *Catal. Lett.* **38**, 149 (1996).
26. Giannantonio, R., Ragaini, V., and Magni, P., *J. Catal.* **146**, 103 (1994).
27. Levy, P.-J., and Primet, M., *Appl. Catal.* **70**, 263 (1991).
28. Christmann, K., and Ertl, G., *Surf. Sci.* **60**, 365 (1976).
29. Christmann, K., Ertl, G., and Pignet, T., *Surf. Sci.* **54**, 365 (1976).
30. Rieck, J. S., and Bell, A. T., *J. Catal.* **96**, 88 (1985).
31. Arai, M., Nishiyama, Y., Masuda, T., and Hashimoto, K., *Appl. Surf. Sci.* **89**, 11 (1995).
32. Foger, K., and Anderson, J. R., *J. Catal.* **54**, 318 (1978).
33. Vaarkamp, M., Miller, J. T., Modica, F. S., and Koningsberger, D. C., *J. Catal.* **163**, 294 (1996).
34. Dalmon, J. A., Mirodatos, C., Turlier, P., and Martin, G. A., *in* "Spillover of Adsorbed Species" (G. M. Pajonk, S. J. Teichner, and J. E. Germain, Eds.), Studies in Surface Science and Catalysis, Vol. 17, p. 169. Elsevier, Amsterdam, 1983.
35. Homeyer, S. T., Karpiński, Z., and Sachtler, W. M. H., *J. Catal.* **123**, 60 (1990).
36. Menon, P. G., and Froment, G. F., *J. Catal.* **59**, 138 (1979).
37. Menon, P. G., and Froment, G. F., *Appl. Catal.* **1**, 31 (1981).
38. Szilagyi, T., *J. Catal.* **121**, 223 (1990).
39. Kramer, R., and Fischbacher, M., *J. Mol. Catal.* **51**, 247 (1989).
40. Dou, L.-Q., Tan, Y.-S., and Lu, D.-S., *Appl. Catal.* **66**, 235 (1990).
41. Kramer, R., and Andre, M., *J. Catal.* **58**, 287 (1979).
42. Den Otter, G. J., and Dautzenberg, F. M., *J. Catal.* **53**, 116 (1978).
43. Kunimori, K., and Uchijima, T., *in* "Spillover of Adsorbed Species" (G. M. Pajonk, S. J. Teichner, and J. E. Germain, Eds.), Studies in Surface Science and Catalysis, Vol. 17, p. 197. Elsevier, Amsterdam, 1983.
44. Knözinger, H., and Ratnasamy, P., *Catal. Rev.-Sci. Eng.* **17**, 31 (1978).
45. Dmitriev, R. V., Detjuk, A. N., Minachev, Ch. M., and Steinberg, K.-H., *in* "Spillover of Adsorbed Species" (G. M. Pajonk, S. J. Teichner, and J. E. Germain, Eds.), Studies in Surface Science and Catalysis, Vol. 17, p. 17. Elsevier, Amsterdam, 1983.